



Carbon enhanced cementitious coatings: Alternative anode materials for impressed current cathodic protection systems intended for reinforced


Downloaded from: <https://research.chalmers.se>, 2025-12-05 01:47 UTC

Citation for the original published paper (version of record):

Jansson, H., Zhang, X., Ye, L. et al (2024). Carbon enhanced cementitious coatings: Alternative anode materials for impressed current cathodic protection systems intended for reinforced concrete. *Materials and Corrosion - Werkstoffe und Korrosion*, 75(6): 705-718. <http://dx.doi.org/10.1002/maco.202314178>

N.B. When citing this work, cite the original published paper.

Carbon enhanced cementitious coatings: Alternative anode materials for impressed current cathodic protection systems intended for reinforced concrete

Helen Jansson¹ | Xiaoyan Zhang² | Lilei Ye³ | Luping Tang¹ | Amir Saeid Mohammadi¹ | Arezou Babaahmadi¹ 

¹Department of Architecture and Civil Engineering, Chalmers University of Technology, Gothenburg, Sweden

²Department of Chemistry and Chemical Engineering, Chalmers University of Technology, Gothenburg, Sweden

³Chalmers Industriteknik, Gothenburg, Sweden

Correspondence

Arezou Babaahmadi, Department of Architecture and Civil Engineering, Chalmers University of Technology, 412 96 Gothenburg, Sweden.
Email: arezou.ahmadi@chalmers.se

Funding information

Materials Science Area of Advance at Chalmers; Strategic innovation program SIO Grafen; Sweden's innovation agency (Vinnova)

Abstract

In this study, the functionality of self-formulated carbon-based conductive coatings (CBCCs) with incorporation of graphite as the anode in an impressed current cathodic protection system is studied. The anode materials are tested and evaluated for long-term durability and performance by an accelerated durability test method. The results show that the functional time is highly dependent on the acceleration factor, and thus the charge passed through the material during testing, as well as the material composition. From the results, there are also indications that the addition of graphene into the CBCC matrix has a positive effect on the homogeneity of the material, but without any major influence on the conductivity and performance.

KEYWORDS

accelerated durability test, conductive anode material, conductive coating, graphene, graphite, impressed current cathodic protection (ICCP), long-term performance, scanning electron spectroscopy

1 | INTRODUCTION

Worldwide, infrastructure depends on available and affordable materials. One such material is cement-based concrete, which is most widely used both in terms of volume and mass. However, cement-based materials, like concrete, are

also a significant source of global carbon dioxide (CO₂) emissions. The extensive use of concrete (worldwide ~10 km³^[1–3]) causes high CO₂ emissions not only because of the fossil fuels used for the production of cement, but also due to the large amount of CO₂ released to the air during the calcination process (650–900 kg CO₂/ton clinker).^[4]

Abbreviations: CBCC, carbon-based conductive coating; CemCoat, Lanark micro-cement; GeS, graphene in suspension; GiP, graphite powder; HSA, micro-graphite; ICCP, Impressed current cathodic protection; rGO, reduced graphene oxide; SAC, Lanark Vinnapas 240 D; SBR, Sika SikaLatex; SEM, scanning electron spectroscopy.

This is an open access article under the terms of the [Creative Commons Attribution-NonCommercial-NoDerivs](https://creativecommons.org/licenses/by-nc-nd/4.0/) License, which permits use and distribution in any medium, provided the original work is properly cited, the use is non-commercial and no modifications or adaptations are made.

© 2024 The Authors. *Materials and Corrosion* published by Wiley-VCH GmbH.

One of the solutions to reduce CO₂ emissions from the cement and concrete sector is partial substitution of cement clinker with supplementary cementitious materials, which allows manufacturing and production of concrete in a more sustainable way and has therefore become a common alternative today. However, considering the very large volume of concrete that is needed for infrastructure development and maintenance, sustainability cannot be reached only by reducing the volume of cement used yearly. Also, the service life of concrete-based structures must be extended by, for example, increased durability and long-term performance as well as well-designed repair, maintenance, and service procedures. Thus, for a sustainable construction sector, the primary challenge is to assure the long-term durability, that is, the service life of the materials.

Although concrete itself is a relatively durable material when used under normal exposure conditions, its intrinsic weak tensile strength and cracking sensitivity (e.g., during shrinkage) requires, in most cases, reinforcement, generally in the form of steel bars. However, since concrete structures are porous, they are consequently vulnerable to ingress of aggressive substances such as chlorides. Chlorides are known to induce corrosion of reinforcement, and are therefore also one of the most frequent causes of degradation of steel reinforced concrete structures.^[5] Chloride ions can come from, for example, seawater or de-icing salt, which makes structures in marine environments, such as bridges, or in climates with large temperature fluctuations (where de-icing by salts is the general solution), most prone to this problem. In addition, to extend the service life of concrete-based structures, there are several parameters to consider when choosing a repair technique such as the

extent and severity of the damage, weight limitations, costs, additional maintenance, traffic administration during repairs, esthetics and technical limitations.^[6] This makes the annual cost of corrosion of reinforcement, worldwide, is high and estimated to be 3%–4% of the gross domestic product (GDP) of industrialized countries.^[7,8]

One method to prevent chloride induced corrosion of reinforcement is to cast a thicker cover layer of concrete or to use more dense concretes with lower permeability.^[9,10] However, since such solutions result in both higher costs of the construction as well as use of larger amounts of cement, the consequence is a higher environmental footprint.

Another powerful and effective technique to reduce the cost for prevention of chloride induced corrosion of reinforcement is cathodic protection.^[9,11] Impressed current cathodic protection (ICCP) is a method that can be used to prevent corrosion and to address significant corrosion issues in larger structures.^[12] In such a system the metal surface, that is, the steel reinforcement, acts as the cathode in an electrochemical cell. The anode, to which an electric power is applied, is placed on the surface of the concrete structure. The electric power provides the current that leads to the electrochemical reaction required for the cathodic protection to take place. An ICCP system can be used to control corrosion at any chloride level due to the possibility to alter the applied current, and therefore such a system can be implemented and tuned to the desired protection requirements.^[13]

A schematic illustration of the basic elements of an ICCP system with its external anode and internal cathode is shown in Figure 1. As shown, the anode (the positive terminal) is connected to the positive terminal of a

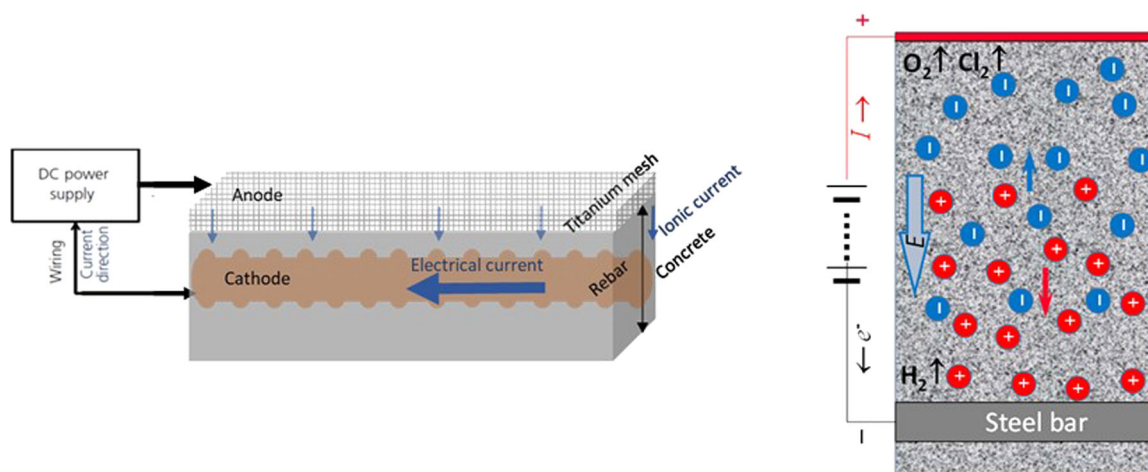
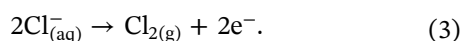
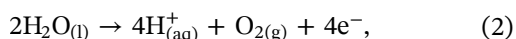
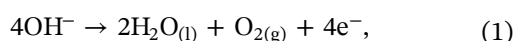


FIGURE 1 To the left, the traditional ICCP system set-up with a titanium mesh as the anode (positive terminal) and the steel reinforcement as the cathode (negative terminal). To the right, a schematic illustration of the cathodic and anodic chemical reactions in an ICCP system. [Color figure can be viewed at wileyonlinelibrary.com]

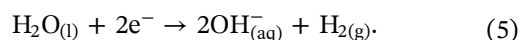
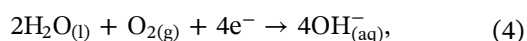
low-voltage DC source and the cathode (the negative terminal) is connected to the reinforcement. Once applied, the IPCC system is expected to operate for the entire service life, and for a proper function, the anode not only has to be a good electrical conductor, but also resistant to corrosion and able to tolerate high currents without forming resistive oxide layers.^[9,12] Examples of ICCP anode materials are magnetite, carbonaceous materials (generally graphite), high-silicon iron (alloy containing silicon), lead/lead oxide, lead alloys and platinised materials such as titanium,^[11] where the latter is the most commonly used anode material.

When a voltage is applied to the ICCP system, several chemical reactions occur and electrons flow to the cathode (i.e., the steel/concrete interface) and induces a cathodic reaction in which hydroxide ions are produced from oxygen and water. The hydroxide ions then migrate through the concrete to the concrete-anode interface, oxidizing to oxygen and electrons, as shown in Equation (1). Other chemical reactions occurring at the cathode and the concrete-anode interface are shown in Equations (2)–(5).

Reactions at the anode:



Reactions at the cathode:



However, although the need for prevention and repair of chloride induced corrosion on reinforcement is extensive, the ICCP system is losing the market due to some major issues related to the anode materials. The main obstacles are high material costs, installation difficulties, and demanding maintenance of the ICCP system.^[14] Furthermore, the installed anode material generally requires a relatively thick (typical on the centimeter scale) cementitious overlay,^[15] which makes the system heavy. Failure of these types of anodes is typically due to disbandment of the overlay, which requires additional repair and maintenance.^[15]

Instead of installation of a metal mesh as the anode in an ICCP system (see Figure 1) also conductive coatings can be used. From such studies^[16–18] it is clear that the main challenge is to create a conductive coating material that not only maintains its functionality in the alkaline concrete environment, but also withstands external environmental

conditions, such as rain or splashes, and exhibits resistance towards consequences of ICCP chemical reactions. Especially the effect on the anode is of importance for the service life and performance.^[19] Also, the gas production during the chemical reactions at the anode (see Equations 1–3) has to be considered, and the coating thus needs to be porous enough to release the gas to avoid damages like delamination of the coating material from the substrate.^[9] In addition, delamination can occur due to the production of hydrogen ions (H^+), which generates an acidic environment, and can lead to a lower Ca/Si ratio and increased porosity of the cementitious matrix,^[20] around the anode. Delamination is thus the most critical parameter to consider when accounting for the service life and durability of the coating material. In the literature there are several studies investigating conductive coating materials, see for example, Refs,^[16–18,21] but very few evaluate the long-term performance. In fact, not even a patented conductive coating material for the anode of an ICCP system^[22] is assessed for long-term performance.

In this study a new type of carbon-based conductive coatings (CBCC) was developed for the utilization as an anode material in an ICCP system to replace the titanium mesh generally used (see Figure 1) with the aim to reduce both cost and time for installation as well as the maintenance to increase its long-term performance and, thereby, its service life. For the development, highly conductive carbon-based materials based on graphite with the addition of smaller amounts of graphene were evaluated for their conductive properties.

The evaluation of the developed CBCCs was performed in three steps: (i) production and evaluation of potential alternatives of CBCCs with different material compositions, (ii) development of a simple conductivity measurement test method for fast screening of the conductivity levels of these material compositions, and (iii) development of an acceleration test to demonstrate the effective service life of the materials, that is, the expected time for the material to be functional. From the results it is obvious that not only the type of graphite but also the binder material used for the CBCC is of importance. In addition, the results indicate that a smaller content of graphene added to the matrix has a positive effect on the homogeneity of the material, however without any major influence on the conductivity.

2 | MATERIALS

For the development of a new type of conductive coatings for the use as the anode in an IPCC system, three types of commercially available carbon-based products from the

Talga group^[23] were investigated. Two of the products were graphite in the form of platelets but with different surface areas. A high surface area micro-graphite (HSA) and a graphite powder (GiP). The third product was a product consisting of graphene nanoplatelets in a water-based suspension (GeS). Information on the products is given in Table 1.

The binder material for the anode, that is, the material in which the carbon-based materials are incorporated were primers produced by Lanark and Sika, respectively. The product from Lanark was a styrene-acrylate copolymer, Vinnapas 240 DH (SAC), and the product from Sika, SikaLatex, was a styrene butadiene rubber (SBR). In addition, a cement-based binder material, a polymer enhanced micro cement from Lanark, was also evaluated (CemCoat).

Based on these products, several CBCCs, with various combinations and amounts of the carbon-based and binder materials, were prepared and evaluated based on the conductivity level (by a fast screening method, see Section 3.1), the porosity and the water resistance. Only combinations with a conductivity of about 1–100 S/m

were considered for testing as the anode in the ICCP system. Details about the material compositions are given in Tables S1–S8.

The cement used for the cementitious substrate on which the CBSS was placed was made of ordinary Portland cement (CEM II/A-LL 42.5 R from Heidelberg Cement group), the material chemical composition is shown in Table S9. Each substrate was in the form of a prism with the dimensions $40 \times 40 \times 160$ mm. For the investigations a series of specimen was made, each consisting of a cementitious substrate covered with the developed CBCC, that is, the conductive anode material. The CBCC was, in turn, covered by a thin protective cementitious layer.

3 | METHODS

3.1 | Conductivity measurements

A simple test method for fast screening of the conductivity level of the anode materials was developed, the set-up is illustrated in Figure 2. As shown, the cementitious

TABLE 1 Material specification of the carbon-based materials.

Material	Bulk density (g/cm ³)	Surface area (m ² /g)	Lateral size D10 (μm)	Lateral size D50 (μm)	Lateral size D90 (μm)
HSA	0.15–0.25	25–35	1–3	3–6	7–11
GiP	0.3	6.1	2.4	5.5	12.1
GeS			<0.1	<0.13	<2

Note: The lateral sizes were determined by laser scattering and the surface area by BET.

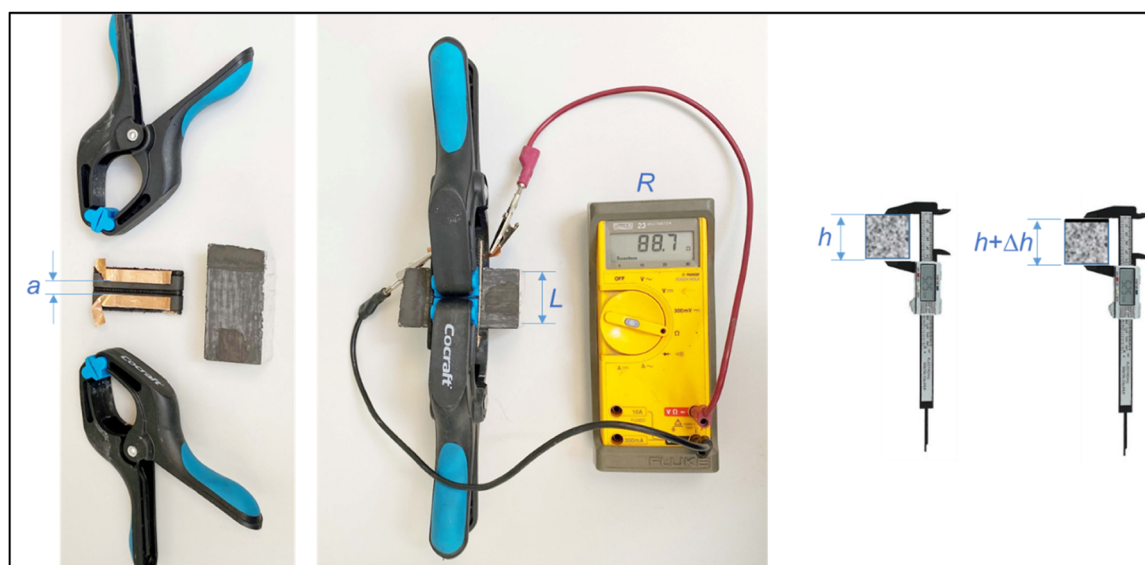


FIGURE 2 The set-up for fast screening of the conductivity level of the anode material. [Color figure can be viewed at [wileyonlinelibrary.com](https://onlinelibrary.wiley.com/doi/10.1002/maco.202314178)]

substrate, coated with the CBCC, is connected to a voltmeter by two cables, which, in turn, are connected to the coating by two copper tapes. To secure the contact between the copper tapes and the coating material two clamps were used. The resistivity and conductivity are calculated according to Equations (6) and (7), respectively.

$$\text{Resistivity } (\rho) = R \times L \times Dh/a, \quad (6)$$

$$\text{Conductivity } (\sigma) = 1/\rho, \quad (7)$$

where R is the resistance measured by a common voltmeter, L is the width of the sample, Δh is the thickness of the conductive coating and a is the distance between copper tapes.

3.2 | Durability test method

To evaluate the service life of the developed conductive coatings, that is, the CBCCs, an accelerated durability test method was used. As shown by the schematic illustration of the arrangement in Figure 3, the cementitious substrate, coated with one of the developed CBCCs, was placed on a stainless-steel plate holder in a plastic container, which was partially filled with a 10% NaCl solution. Thus, part of the cementitious substrate was submerged into the solution and part of it, including the conductive coating, was kept above the solution. With this arrangement, the stainless-steel plate functions as the cathode of the electrochemical cell and is thus connected to the negative terminal of a power supply. The CBCC functions as the anode and is therefore connected to the positive terminal of the power supply. The connection was secured through the fixation of a

carbon brush on the CBCC through which the connection to the power supply is obtained, see Figure 4.

In general, the recommended applied current density for prevention of corrosion of steel reinforcement of concrete structures is 2 mA/m^2 (EN 12696-1). However, by applying higher levels of the current density at varying time durations it is possible to accelerate the process and evaluate the functionality over time.^[24] In Table 2 the applied current densities, the duration in terms of experimental time and the corresponding real time, and the calculated acceleration factor are presented.

3.3 | Microscopy: Scanning electron microscopy

The surface topography and elemental composition of the CBCC and the concrete-anode interface were analyzed by use of scanning electron microscopy (SEM). For the investigations, a FEI Quanta ESEM 200 equipped with a field emission gun and an Oxford Inca energy dispersive X-ray (EDX) system was applied on thin cubes of the solid sample with a dimension of about $20 \times 10 \times 10 \text{ mm}$. Before the measurements, the samples were vacuum dried and polished. The chemical analysis by EDX was performed in high vacuum mode and at a 9.5 mm working distance.

3.4 | Pull-off test

The adhesive connection between the surface of the cementitious substrate and the CBCCs was measured by a pull-off test. This is a near-to-surface method, which measures the resistance of the coating, in this case the anode material, to separate from the substrate when a

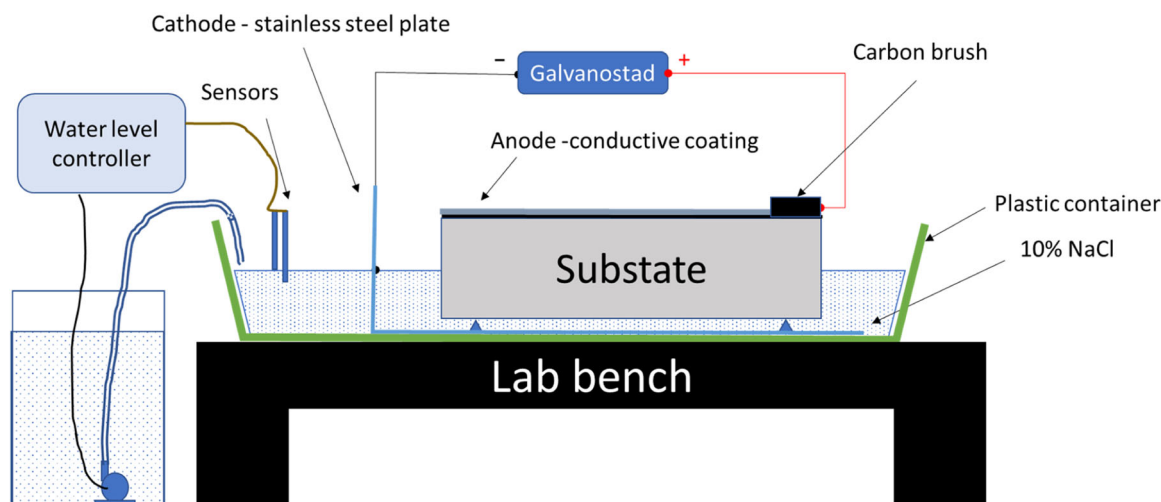


FIGURE 3 The set-up for the durability test by the ICCP method. [Color figure can be viewed at [wileyonlinelibrary.com](https://onlinelibrary.wiley.com/doi/10.1002/maco.202314178)]



FIGURE 4 Photos showing the placement of the carbon brush and its connection to the conductive coating (CBCC). [Color figure can be viewed at [wileyonlinelibrary.com](https://onlinelibrary.wiley.com/doi/10.1002/maco.202314178)]

TABLE 2 Specification of accelerated durability test method parameters.

Applied current density	Experimental time versus real time	Acceleration factor
730 mA/m ²	1 day testing = 1 year	365
104 mA/m ²	1 week testing = 1 year	52
26 mA/m ²	4 weeks testing = 1 year	13

perpendicular tensile force is applied. The results are thus given by the force required to pull the conductive coating layer from the surface of the substrate. The set-up is schematically illustrated in Figure 5.

4 | RESULTS AND DISCUSSION

4.1 | Characteristics of the coating systems

Figure 6 presents the conductivity levels of the CBCCs (presented in Table 3) as a function of graphite content. As can be observed, in terms of the measured conductivity level the CBCCs can be divided into three groups. One group, marked by a blue dashed line, is the primer-based (i.e., SAC of SBR) anode. Among the CBCCs, these materials show the highest conductivities at the lowest carbon content and the conductivity level appears to be dependent on the carbon content since there are indications that a small increase in graphite content results in a relatively large increase in conductivity. The

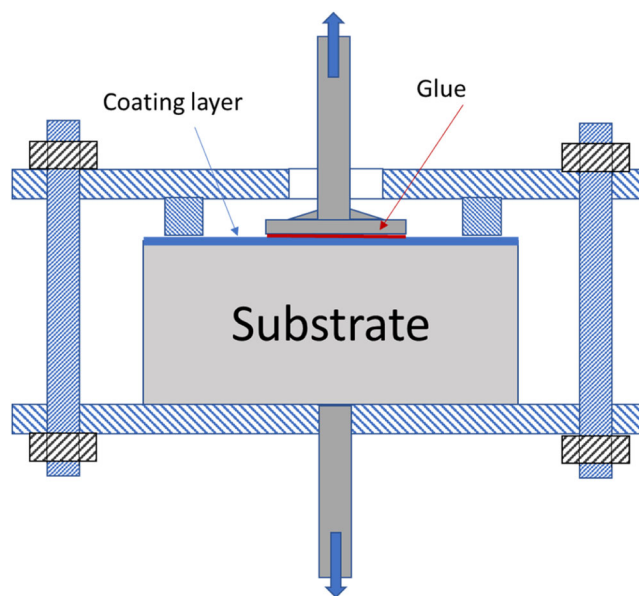


FIGURE 5 A schematic illustration of the set-up for the pull-off tests. [Color figure can be viewed at [wileyonlinelibrary.com](https://onlinelibrary.wiley.com/doi/10.1002/maco.202314178)]

group marked by a red dotted line shows the mineral-based (CemCoat) CBCC, which in comparison with the CBCCs based on the primer materials, generally shows lower conductivity even if the carbon content is higher. For this CBCC, an increased graphite content results, as expected, in an increase in the conductivity, however, with a less pronounced effect than that obtained for the primer-based CBCCs.

The third group, marked by a solid green line, are the ternary anode materials HSA + CemCoat + SAC and GiP + CemCoat + SAC. This group of conductive coatings shows among the highest values of the conductivity

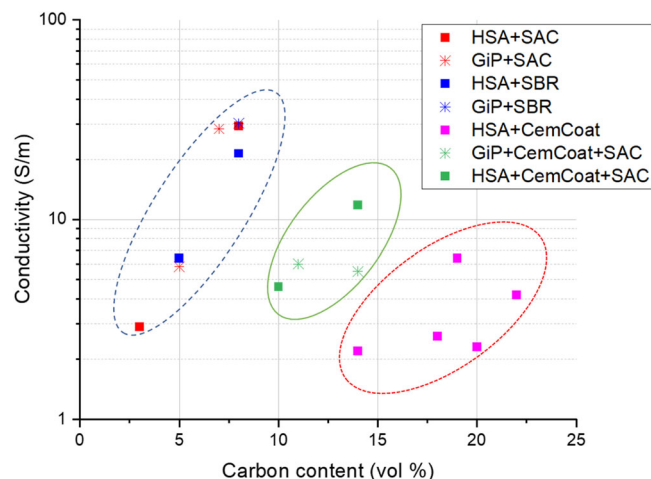


FIGURE 6 Conductivity as a function of the content of carbon-based material in developed coating systems. The blue dashed line shows the group of water resistant and gas permeable anode materials and red dotted line the group with opposite properties. [Color figure can be viewed at [wileyonlinelibrary.com](https://onlinelibrary.wiley.com/doi/10.1002/maco.202314178)]

TABLE 3 Evaluation of the water resistance and gas permeability of the hypothetical coating systems.

Coating material	Water resistance	Gas permeability
1. HSA + SAC	✓	X
2. GiP + SAC	✓	X
3. HSA + SBR	✓	X
4. GiP + SBR	✓	X
5. HSA + CemCoat	X	✓
7. HSA + CemCoat + SAC	✓	✓
8. GiP + CemCoat + SAC	✓	✓

Note: ✓ indicates positive and X negative results, respectively.

at intermediate contents of graphite within the evaluated interval (i.e., at lower and higher carbon content than the CemCoat and the primer-based CBCCs, respectively). Worth mention is that also fast screening of a CBCC with graphene (in the form of reduced graphene oxide, rGO, described in Table S6) incorporated in the CemCoat matrix was evaluated, but the results showed on a very low conductivity level (~ 0.25 S/m), and therefore this CBCC was excluded from further investigations. Such a result is unexpected and in contrast to most of the existing literature, see, for example, Refs.^[25,26] The reason for this is not clear but it can be due to that the addition of rGO to the cementitious material, like the here used CemCoat, can result in a decrease in conductivity due to that the particles increase the gel pore structure, which decreases the mean free path for electron transmission and, thereby, increases the electric

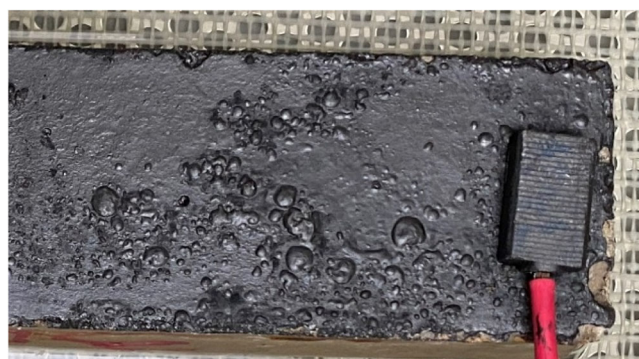


FIGURE 7 Gas bubbles generated at the anode, and how it affects the surface of coating systems with low gas permeability. [Color figure can be viewed at [wileyonlinelibrary.com](https://onlinelibrary.wiley.com/doi/10.1002/maco.202314178)]

resistivity.^[26] Another possible explanation is that rGO tends to agglomerate in an alkaline environment.^[27]

As mentioned above, in addition to the conductive properties of the developed CBCC, also the gas permeability of the material as well as its resistivity towards water are of great importance.^[9] A porous structure is crucial for the release of the gases generated around the anode during the anode reactions (see Equations 1–3). The ability to resist water is significant to withstand external environmental conditions, like rain or splashes. The developed conductive coatings were therefore characterized with respect to such properties. The gas permeability and water resistance were evaluated after conductivity measurements for 1 week with an applied current density of 2 mA/m^2 . The water resistivity was thereafter evaluated based on whether the coating could be easily washed off the cementitious substrate, and the gas permeability was assessed with respect to effect on the coating due to gas production and accumulation during the conductivity measurements.

The water resistance and gas permeability properties of the CBCCs are shown in Table 3. As observed, the CBCCs based on only a primer as the binder material (Samples 1–4, based on either SAC or SBR) display a good resistance towards water but show negative results in terms of gas permeability. Although the final product was not exactly easy to wash off, that is, removed from the concrete surface (i.e., the substrate) by water, the conductive coating displayed a very short time of function due to delamination from the substrate caused by the poor gas permeability. One typical example of this is presented in Figure 7, where it can be observed that the CBCC is destroyed by the generated gas. The reason for this is that the anode material has poor gas permeable properties, which results in that gas generated during the anodic reactions (Equations 1–3) cannot be released. This, in turn, results in blisters and delamination of the

anode and, consequently, to the end of the service life of the primer-based CBCCs.

The CBCC with the mineral-based binder (CemCoat) displays the opposite behavior to the primer-based anodes, see Table 3. Even if this type of binder materials can release the gas generated during the anodic reactions, it shows a very weak water resistance. In addition, the CBCC is easily brushed away from the substrate directly during use. Only two of the possible anode materials show the desired and required properties, that is, suitable properties in terms of both gas permeability and water resistance. These are the ternary conductive coatings HSAS + CemCoat + SAC and GiP + CemCoat + SAC.

As shown in Figure 6, there is a difference in the conductivity level of these ternary CBCCs, especially at higher graphite contents, which partly can be explained by that the surface area of HSA is larger than that of GiP (see Table 1). The reason for the variations in conductivity with relatively small variations in graphite content, seen for the CBCC HSA + CemCoat + SAC, may be due to small variations in thickness of the conductive coating, or that the combination of CemCoat with SAC or SBR, makes the structure both porous, and thereby gas permeable, as well as reasonable water resistant as discussed above and shown in Table 3. Since conductivity is dependent on the porosity,^[28,29] one explanation for the difference in conductivity is the difference in porosity, and consequently the ionic conductivity properties,^[30] of the CBCC for mineral binder material compared to the primer-based CBCCs. Another explanation can be that there is an optimum content of graphite for the conductivity, as previously shown for a conductive anode material with incorporated graphite.^[31]

4.2 | Conductive composite coatings for the anode

Based on the results presented in the previous section, it is obvious that only two of the possible anode materials show all the desired and required properties, that is, proper

properties in terms of both gas permeability, water resistance, and conductivity, that is, the ternary coating materials HSA + CemCoat + SAC and GiP + CemCoat + SAC. In addition to these ternary CBCCs, two additional material compositions, with the addition of smaller amounts of graphene (GeS) were prepared to further screen the effects (see Tables S5 and S7). Thus, four material compositions, which are described in Table 4, and hereafter denoted C1, C2, C3, and C4, were prepared for further investigations. Worth noting is that the introduction of graphene (GeS) resulted in a reduction of the conductivity level, see Table 4, which is highly unexpected since graphene has superior conductive properties compared to graphite. The reason for this is unclear but one explanation could be that graphene is not homogeneously distributed in the CBCCs, which should affect the network structure necessary for high conductivity. Also, as can be observed from the table is that the reduction in conductivity is higher for the CBCC containing GiP than for the one containing HSA, which most likely depends on the fineness and surface area of the graphite. However, as found from the investigations, when graphene is added to the CBCC there is a general enhancement in the more macroscopic homogeneity of the material, which is expected to have a positive influence of the material performance. The homogeneity of these CBCCs is discussed below in Section 4.3.

4.3 | Accelerated durability tests of the developed conductivity anode materials

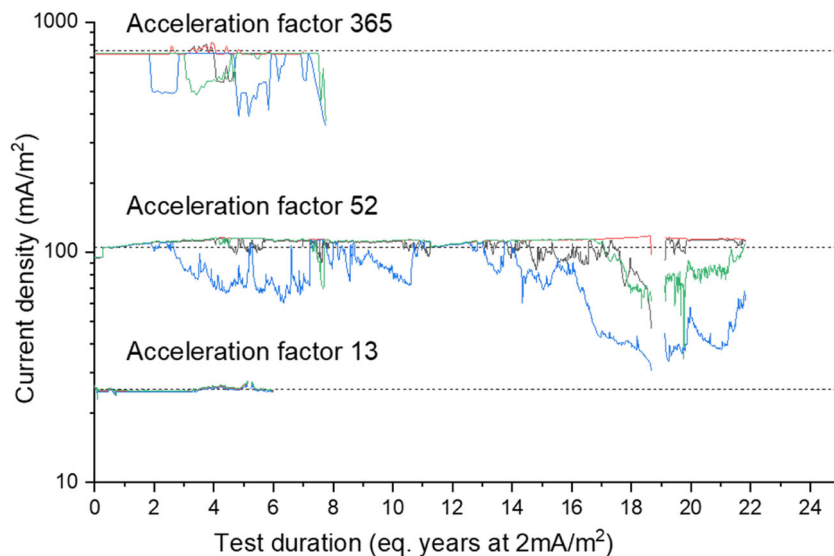
In Figure 8 the applied current density through the anode during the accelerated durability tests, by the different acceleration factors, as a function of the corresponding duration time (given in eq. years, see Table 2), is shown for the CBCCs C1, C2, C3, and C4 described in Table 4. For zoom-in figures of the results, on a linear scale, see Figures S1–S3. From the results it is clear that when subjected to the highest applied current density, that is, 730 mA/m², (acceleration factor 365) the current density through the materials starts to deviate

TABLE 4 The material compositions and the conductivity obtained by the fast-screening method of the investigated conductive coatings (the CBCCs).

Denotation	Material composition	Content (g)	Conductivity (S/m)
C1	HSA + CemCoat + SAC	150 + 100 + 250	15.5
C2	HSA + GeS + CemCoat + SAC	150 + 1.25 + 100 + 250	13.1
C3	GiP + CemCoat + SAC	150 + 100 + 250	13.55
C4	GiP + GeS + CemCoat + SAC	150 + 1.55 + 100 + 310	6.0

Note: The water/material-ratio is for all compositions ~0.5.

FIGURE 8 The current densities through the anode as a function of duration time (in equivalent years). The results for CBCCs C1, C2, C3, and C4 are shown by black, red, blue, and green lines, respectively. The dashed lines are only a guide to the eye. Note that the result for acceleration factor 13 is not complete, these measurements are still ongoing. [Color figure can be viewed at [wileyonlinelibrary.com](https://onlinelibrary.wiley.com/doi/10.1002/maco.202314178)]



from the applied current density after a rather short functional time, corresponding to approximately 2 equivalent years. From the results it is also indicated on that the drop in conductivity occurs earliest for the CBCC C3. The deviation from the applied current density for CBCCs C4 and C1 starts at around 3 and 4 equivalent years, respectively. Subjected to this high acceleration factor, C2 seems to be the most resistant anode material against resistivity increases and material damages. The 730 mA/m² ICCP acceleration was interrupted at an equivalent time corresponding to approximately 8 years because the resistance of the anode materials became too high, and the materials was thus no longer considered functional.

For CBCCs subjected to the acceleration factor 52 (i.e., an applied current density of 104 mA/m²) the same scenario as for acceleration factor 365 is observed. There is, thus, a start of deviation from the applied current density at about the same equivalent years for the different CBCCs as for the higher acceleration factor. Here it should be noted that also for an applied current density of 104 mA/m², the conductive coating C2 is the most resistant material. The experiment was interrupted after an equivalent time of about 22 years.

The possible microstructural changes within the anode materials as well as around the anode that give rise to the reduced conductivity with time, during the durability tests with accelerations factors 365 and 52, is further discussed in the next section.

As also can be observed in Figure 8 (and Figure S3), the ICCP accelerated durability test with the lowest applied current density, that is, 26 mA/m² (acceleration factor 13) results in a completely different scenario compared to the higher acceleration factors. This experiment is still ongoing and at the present time, which is equivalent to approximately 6 years,

there is no indication of a drop in conductivity for any of the CBCCs. Worth noting is also that this acceleration is 13 times higher than the recommended applied current density (2 mA/m²) for corrosion prevention of steel reinforcement. This implies that the developed CBCCs can be considered as highly stable materials since they can withstand this rather high applied current density and thus, making them suitable as the anode in an ICCP system.

Figure 9 shows the total charge passed through the CBCCs during time of exposure to the applied current densities. For the CBCCs subjected to the highest applied current density (red bars in the bar chart) the mean value of the charge passed is ~0.49, ~0.54, ~0.52, and ~0.57 MC for the material combinations C1, C2, C3, and C4, respectively, after an equivalent time of 8 years. For the medium acceleration factor (blue bars) the corresponding charge passed is ~1.39, ~1.48, ~1.06, and ~1.39 MC at a time duration of approximately 22 years.

For the lowest acceleration factor (green bars) the charged pass after an equivalent time of 6 years is about the same for all anode material compositions, ~0.36 MC. However, as mentioned above, these measurements are still ongoing and since there is no sign of any changes in conductivity, a much higher value of charged passed through the material is expected when the experiment is terminated.

Previous studies have shown that the applied current density plays the most important factor for the service life of the anode.^[30,32] A higher applied current density results in a higher total charge passing through the anode during the ICCP functional time and a resistivity increase around the anode.^[30] This, in turn, decreases the efficiency of the anode, which with time results in a complete destruction of the material. An important

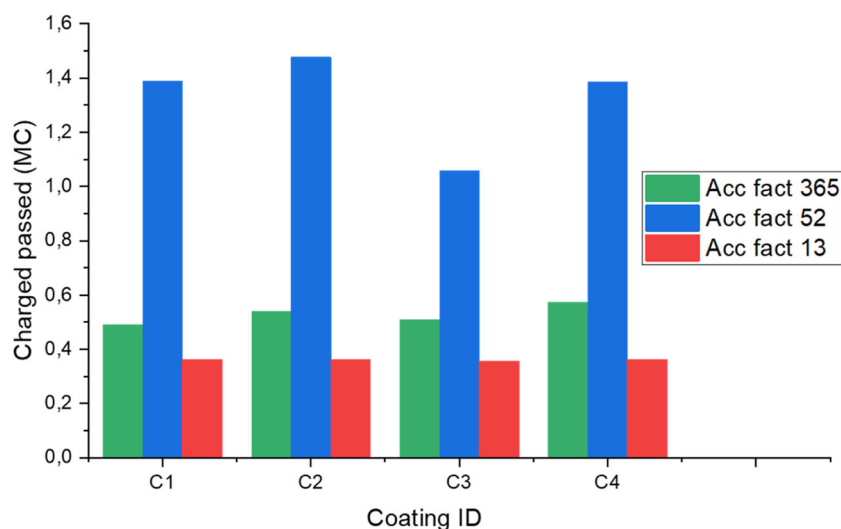


FIGURE 9 The total charge passed through the conductive anode materials (coating ID, see Table 3) during the experimental time. [Color figure can be viewed at [wileyonlinelibrary.com](https://onlinelibrary.wiley.com/doi/10.1002/mco.2023.14.78)]

observation from Figure 9 is also that the CBCCs C2 and C4 display the highest values of the charge passed both at the highest and medium levels of the accelerations tested. This is most likely due to that these material compositions are the most homogeneous of the CBCCs, which will be discussed in more detail in Section 4.4 below.

4.4 | Microstructural characterization

Figure 10 shows the SEM images of the developed CBCCs and as can be observed, there is a rather large difference in homogeneity between the different material combinations. The CBCCs that appear to be the most homogeneous are C2 and C4, that is, the materials to which a smaller amount of graphene (GeS) is added. Of these two CBCCs, the most homogeneous is C2, which is also the anode material that is most resistant to the highest applied current densities (acceleration factors 52 and 365) as shown in Figure 8. Due to its homogeneity and the very promising results from the acceleration tests, the conductive coating C2 was the focus for further evaluation.

To evaluate the effect of the accelerated IPCC, that is, the applied current density, on the microstructure of the CBCC and the anode-concrete interface in more detail, the conductive coating C2 subjected to the highest acceleration factor (hereafter called C2-365) was evaluated in comparison with a reference consisting of the same anode material but without any applied current density, that is, with an acceleration factor of 0 (hereafter called C2-0). The results are shown in Figure 11. Based on the image of C2-0 (Figure 11a), three layers are easily seen, the concrete substrate, the conductive anode layer (black part), and the thin protective layer of cement

coating (without any incorporation of graphite or graphene). This contrasts however with the image representing C2-365 (Figure 11b).

When subjected to this high applied current density, it is obvious that an additional layer is built up between the anode material and the concrete cover. This layer is due to that a very large amount of gas is generated during the anodic reactions when the material is subjected to such a high acceleration factor. Even if the material is reasonably gas permeable, such large amounts of generated gas cannot be released to the surrounding area. Instead, part of it is accumulated, which affects the structure, and an additional porous layer is built up at the anode-concrete cover interface. This layer is, however, not expected to have any effect on the conductivity of the CBCC, or the resistivity of the concrete substrate, but only affect the cementitious cover layer.

As shown in Equation (2), one of the chemical reactions at the anode results in production of hydrogen ions, that is, a pH decrease. Such acidification is well known to be associated with the applied current density and the total charges passed through materials during time of exposure.^[30] In addition, it is well known that increased acidity leads to leaching of calcium in porous layer between the anode and the concrete substrate, which, in turn, causes an increase in the resistivity at the interface between the anode and concrete substrate.^[30,33] From the SEM image of C2-365 there are indications on a thin porous layer at the interphase between the substrate and the CBCC layer, see marked area in Figure 11b (for an enlargement of this image, see Figure S4). This porosity is most likely caused by leaching of calcium. Moreover, when compared to C2-0 there are also indications on a somewhat higher porosity of the conductive coating layer of C2-365, which also can affect the conductivity level due to the influence on the carbon network.

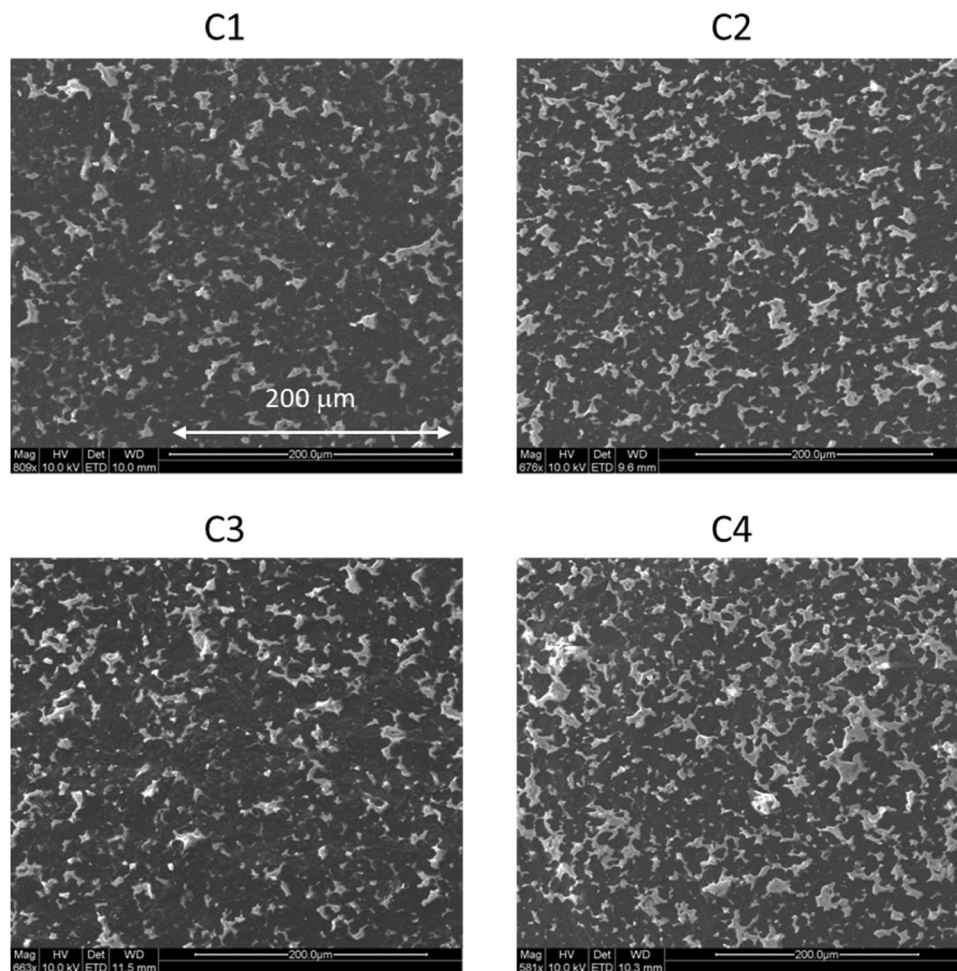


FIGURE 10 SEM images of the surface of the developed anode materials C1, C2, C3, and C4.

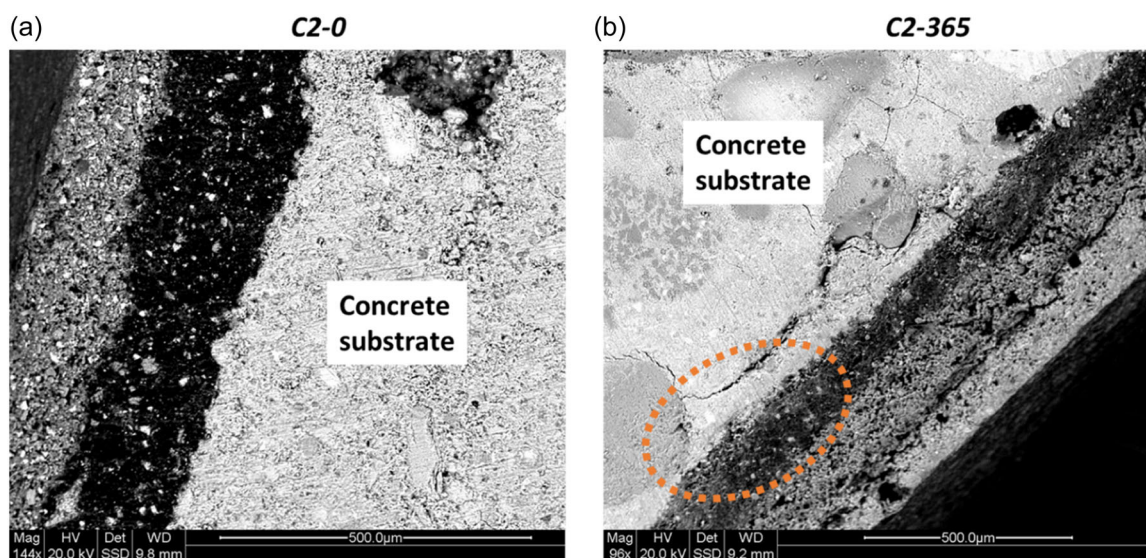


FIGURE 11 A comparison of the microstructure with (a) and without (b) an applied current density. The dashed circle shows the porous zone at the interface between the CBCC layer and the cementitious substrate. [Color figure can be viewed at [wileyonlinelibrary.com](https://onlinelibrary.wiley.com/doi/10.1002/maco.202314178)]

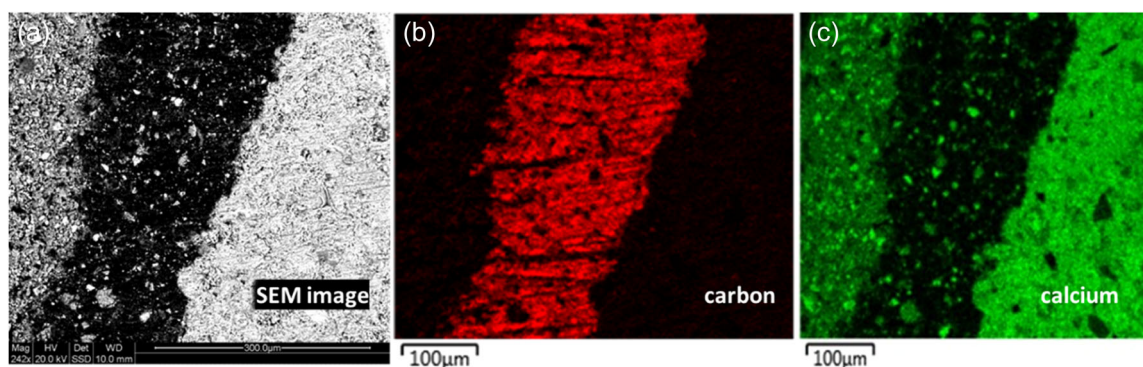


FIGURE 12 (a) SEM image of C2-0 and EDX analysis of the carbon (b) and calcium (c) at the different layers of the system. The cementitious substrate is to the right and the thin cover layer to the left in the images. The conductive coating is the dark (black) layer in image a. [Color figure can be viewed at [wileyonlinelibrary.com](https://onlinelibrary.wiley.com/doi/10.1002/maco.202314178)]

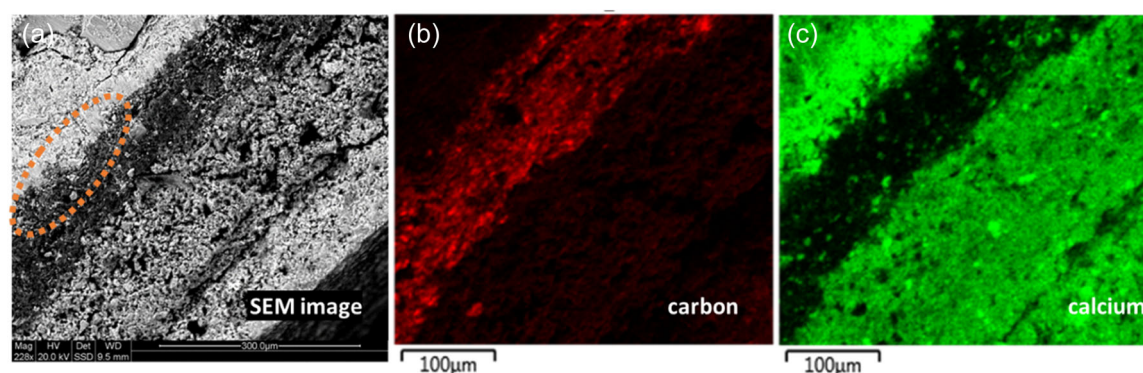


FIGURE 13 (a) SEM image of C2-365 and EDX analysis of the carbon (b) and calcium (c) contents at the different layers of the system. The cementitious substrate is to the left and the thin cover layer to the right in the images. The conductive coating is the dark (black) layer in image a. The dashed circle shows the porous part of the zone between the substrate and the CBCC. [Color figure can be viewed at [wileyonlinelibrary.com](https://onlinelibrary.wiley.com/doi/10.1002/maco.202314178)]

To further investigate the microstructure and microstructure changes, elemental composition of the different layers was investigated by energy-dispersive X-ray spectroscopy (EDX). The results are presented Figures 12 and 13. The SEM images on which EDX analysis were performed is shown in Figure 12a (C2-0, i.e., the reference) and 13a (C2-365) and Figures 12b,c and 13b,c the elemental analysis of the same materials.

Concentrating on the anode layer for C2-0, that is, the middle layer (black area) in Figure 12a, it is obvious that this layer, as expected, contains large amounts of carbon (Figure 12b) and only smaller amounts of calcium (Figure 12c). The concrete substrate and the thin cementitious cover layer mainly consist of calcium. This is an expected result since the specimen is not subjected to an applied current density, and thereby there is no expected gas production that can have negative effects on either of the materials or the interfaces at the anode.

Figure 13 shows the corresponding results for C2-365, that is, the specimen subjected to the highest applied

current density. From the results, it is obvious that the anode layer of C2-365 is intact since no larger amounts of calcium are present (Figure 13c). However, in comparison with Figure 12, the CCBC layer of C2-365 seems to be somewhat more porous and/or diffused (for an enlargement of Figure 13a, see Figure S4). However, as expected also in this case the anode layer consists mostly of the carbon-based materials used for the development of the CBCC. Also expected is the presence of calcium in the thin concrete cover layer. However, as shown in Figure 13a (and enlarged in Figure S4) there are some cracks in the cementitious substrate and a porous zone between the cementitious substrate and the conductive coating that is not seen for C2-0 (Figure 12). As discussed above, applying a current density to the system results in gas production and acidification at the anode. The higher the applied current density, the more gas is produced and the higher the acidification.^[34] The acidification has a direct effect on the structure since it consumes calcium hydroxide (CaOH, Portlandite), where an increase in

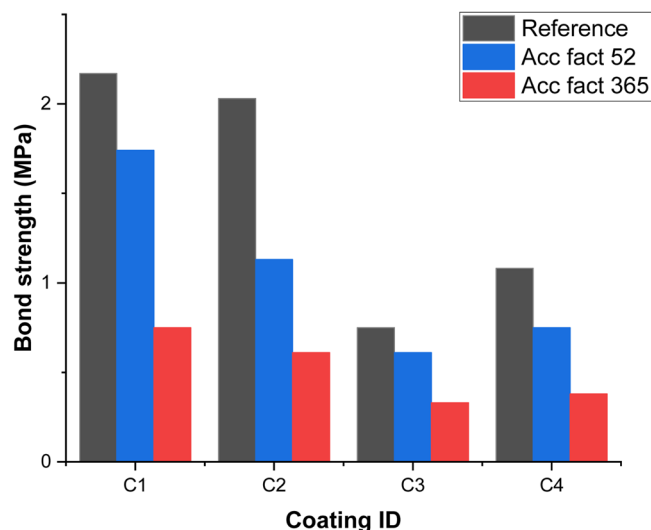


FIGURE 14 Bar chart showing the pull-off test results for the material compositions C1, C2, C3, and C4 exposed to the acceleration factors 52 (blue bars) and 365 (red bars) in comparison with the material compositions without an applied current density (i.e., acceleration factor 0, gray bars). [Color figure can be viewed at [wileyonlinelibrary.com](https://onlinelibrary.wiley.com/doi/10.1002/maco.202314178)]

acidity eventually destroys the calcium-silicate-hydrate (CSH) gel by calcium leaching and deteriorates the bond strength between the cementitious substrate and the anode.^[35] In accordance with this, the results strongly suggest that the porous zone indicated by the dashed circle in Figure 13a is due to such microstructural changes and also the most likely reason for the increased electrical resistance of the system.

4.5 | Pull-off test

The results of the pull-off test for C1, C2, C3, and C4 subjected to the acceleration factors 52 and 365 are shown in Figure 14 together with the reference materials, that is, the same CBCCs without exposure to any applied current densities. It should here be noted that the material compositions subjected to the lowest current density (acceleration factor 13) is still an ongoing experiment and the results are therefore not included in the figure.

Obviously, there is a rather large difference in the pull-off test results for the reference CBCCs. In the case of the reference material (gray bars) the highest value is obtained for the material composition C1-0 (2.17 MPa) followed by C2-0 (2.03 MPa) and C3-0 and C4-0 (both with the value 0.75 MPa). A similar trend, however, with lower bond strengths compared to the reference, is observed for both the CBCCs subjected to the acceleration factors 52 and 365, shown by blue and red bars,

respectively. The relatively large difference between the ICCP accelerations 52 and 365 can be explained by the difference in the total charge passed through the CBCC (see Figure 9), which is much higher for the acceleration factor 52 than for the acceleration factor 365. Since a bond strength lower than 1 MPa can be considered a failure,^[31] it can be noted that the CBCC combinations C3 and C4 should not be considered for an ICCP system.

5 | CONCLUSIONS

In this study we have investigated and evaluated new types of conductive coatings as the anode for an ICCP system, consisting of a combination of commercially available materials, by an accelerated durability test. The results show that a matrix made of a combination of a micro-cement (CemCoat) and a styrene-acrylate copolymer (SAC) with the incorporation of a micro-graphite together (HSA) with a smaller amount of graphene (GeS) show all the required and desired properties and can withstand relatively high applied current densities. This material, called C2 in the present study, shows proper characteristics in terms of conductivity and water resistance, and it is porous enough to release relatively large amounts of the gases generated during the ICCP anodic reaction. The results also show that the incorporation of smaller amounts of graphene into the cementitious matrix mainly influences the homogeneity of the matrix.

With the developed conductive coatings, the generally costly and time consuming required for the preliminary work, as in the case of installing a titanium mesh, can be avoided. This is expected to reduce not only the labor costs but also the inconvenience of, for example, traffic management during installation. The additional weight of the structure is also considerably minimized as a heavy cementitious overlay will not be required.

AUTHOR CONTRIBUTIONS

Helen Jansson: Writing—original draft, review and editing, data analysis, visualization. **Xiaoyan Zhang:** Methodology, investigation, review and editing. **Lilei Le:** Methodology, investigation, review and editing. **Luping Tang:** Conceptualization, methodology, experimental analysis, visualization. **Amir Saeid Mohammadi:** Experimental analysis. **Arezou Babaahmadi:** Conceptualization, methodology, formal analysis, investigation, writing—original draft, review and editing, visualization, supervision, funding acquisition, project administration.

ACKNOWLEDGMENTS

The authors gratefully appreciate constructive discussion and delivery of raw materials to this work from Lars

Nilsson at Lanark Construction AB, Lucia Lombardi and Karanveer S. Aneja at Talga, Edvin Vesterberg at Gatu och Väg Väst (GVV) and Nelson Silva at Sika as well as Sofia Öiseth at Chalmers Industriteknik. This work is part of the project: Graphene enhanced conductive cementitious coating (GREC) financed by Sweden's Innovation Agency (Vinnova), through the strategic innovation program SIO Grafen, a joint initiative by Vinnova, Formas and the Swedish Energy Agency.

CONFLICT OF INTEREST STATEMENT

The authors declare no conflict of interest.

DATA AVAILABILITY STATEMENT

The data that support the findings of this study are available from the corresponding author upon reasonable request.

ORCID

Arezou Babaahmadi  <http://orcid.org/0000-0002-1911-0272>

REFERENCES

- [1] A. Favier, C. De Wolf, K. Schrivener, G. Habert, *A Sustainable Future for the European Cement and Concrete Industry: Technology Assessment for Full Decarbonisation of the Industry by 2050*, ETH Zurich, Zurich **2018**. https://europeanclimate.org/wp-content/uploads/2018/10/AB_SP_Decarbonisation_report.pdf
- [2] IPCC, Climate change 2022—Mitigation of Climate change, <https://www.ipcc.ch/report/ar6/wg3/>. **2022**.
- [3] K. L. Scrivener, V. M. John, E. M. Gartner, *Cem. Concr. Res.* **2018**, *114*, 2.
- [4] E. Worrell, L. Price, N. Martin, C. Hendriks, L. O. Meida, *Annu. Rev. Energy Environ.* **2001**, *26*, 303.
- [5] D. W. Hobbs, *Int. Mater. Rev.* **2001**, *46*, 117.
- [6] S. R. Pearson, R. G. Patel, Repair of concrete in highway bridges—a practical guide, Transport Research Laboratory, **2002**. URL: <http://worldcat.org/issn/13656929>
- [7] G. Schmitt, M. Schütze, G. F. Hays, E. Wayne-Burns, E. Han, F. Pourbaix, G. Jacobsen, *World Corrosion Organization, New York*, **2009**.
- [8] Central Intelligence Agency (CIA), *The World Fact Book, Country Comparison of GDP*, Fairfax, VA, USA. <https://www.cia.gov/library/publications/the-world-factbook/rankorder/2004rank.html>. (accessed 28/11/2014) **2009**.
- [9] L. Bertolini, B. Elsener, P. Pedersen, E. Redaelli, R. B. Polder, *Corrosion of Steel in Concrete: Prevention, Diagnosis and Repair*, 2nd ed., WILEY-VCH Verlag GmbH & Co. KGaA, Weinheim **2014**.
- [10] H. Justnes, M. O. Kim, S. Ng, X. Qian, *Cem. Concr. Compos.* **2016**, *73*, 316.
- [11] R. Polder, A. Kranjc, J. Leggedor, A. Sajna, G. Schuten, I. Stipanovic, *Guideline for Smart Cathodic Protection of Steel in Concrete: Assessment and Rehabilitation of Central European Highway Structures*, FEHRL, Brussels, Belgium. **2009**. www.fehrl.org
- [12] K. Wilson, M. Jawed, V. Ngala, *Constr. Build. Mater.* **2013**, *39*, 19.
- [13] R. L. Kean, K. G. Davies, *Cathodic Protection, Guide Prepared British Department Trade and Industry*, vol. 2–4, National Physical Laboratory, Teddington, UK. **1981**.
- [14] Transportation Research Board National Academies of Sciences, Engineering, Medicine, *Cathodic Protection for Life Extension of Existing Reinforced Concrete Bridge Elements*, The National Academies Press, Washington, DC **2009**.
- [15] A. Byrne, N. Holmes, B. Norton, *Mag. Concr. Res.* **2016**, *68*, 664.
- [16] K. Darowicki, J. Orlikowski, S. Cebulski, S. Krakowiak, *Prog. Org. Coat.* **2003**, *46*, 191.
- [17] J. Orlikowski, S. Cebulski, K. Darowicki, *Cem. Concr. Compos.* **2004**, *26*, 721.
- [18] M. Poltavtseva, G. Ebell, J. Mietz, *Mater. Corros.* **2015**, *66*, 627.
- [19] G. Qiao, B. Guo, Y. Hong, J. Ou, *Int. J. Electrochem. Sci.* **2015**, *10*, 8423.
- [20] J. Hu, Y. Y. Wang, Z. M. Zhang, W. H. Guo, Y. W. Ma, W. Zhu, J. X. Wei, Q. J. Yu, *Constr. Build. Mater.* **2019**, *229*, 11.
- [21] A. Goyal, H. S. Pouya, E. Ganjian, *J. Mater. Civil Eng.* **2023**, *35*, 14.
- [22] J. J. Fontana, D. Elling, Walter Reams, Electrically Conductive Polymer Concrete Coatings. *Patent Number US 4908157*, **1990**.
- [23] Personal communication: Due to company confidentiality we can not provide more detailed information about the products, but refer to Talga group ltd. <https://www.talgagroup.com>. for further information.
- [24] E. Q. Zhang, L. Tang, D. Bernin, H. Jansson, *Mater. Corros.* **2018**, *69*, 1104.
- [25] N. Zhang, W. She, F. Y. Du, K. L. Xu, *Materials* **2020**, *13*, 19.
- [26] T. S. Qureshi, D. K. Panesar, *Constr. Build. Mater.* **2019**, *206*, 71.
- [27] R. Z. Wang, R. X. Sun, L. C. Zhao, T. T. Zhang, X. Q. Kong, Y. Fu, *J. Build. Eng.* **2023**, *77*, 16.
- [28] H. Choo, J. Song, W. Lee, C. Lee, *Acta Geotechn.* **2016**, *11*, 1419.
- [29] P. K. Sarkar, N. Mitra, *Cem. Concr. Res.* **2021**, *143*, 8.
- [30] C. Andrade, *Cem. Concr. Res.* **1993**, *23*, 724.
- [31] G. B. Wijaya, D. P. Lays, H. H. Tanto, D. Tjandra, *Civil Eng. Dimen.* **2019**, *21*, 84.
- [32] H. Sun, J. Liu, K. Chu, S. A. Memon, Z. Cen, X. Zhang, D. Li, F. Xing, *J. New Mater. Electrochem. Syst.* **2018**, *21*, 103.
- [33] E. Q. Zhang, Z. Abbas, L. Tang, *Constr. Build. Mater.* **2018**, *185*, 57.
- [34] W. H. A. Peelen, R. B. Polder, E. Redaelli, L. Bertolini, *Mater. Corros.* **2008**, *59*, 81.
- [35] L. Tang, E. Q. Zhang, Y. Fu, B. Schouenborg, J. E. Lindqvist, *Mater. Corros.* **2012**, *63*, 1119.

SUPPORTING INFORMATION

Additional supporting information can be found online in the Supporting Information section at the end of this article.

How to cite this article: H. Jansson, X. Zhang, L. Ye, L. Tang, A. S. Mohammadi, A. Babaahmadi, *Mater. Corros.* **2024**, 1–14.
<https://doi.org/10.1002/maco.202314178>